Supporting information

Tunable Thiophene-Based Conjugated Microporous Polymers for the Disposal of Toxic Hexavalent Chromium

Mohammed G. Kotp,[a] Nagy L. Torad,*[b,c] Hiroki Nara,[b] Watcharop Chaikittisilp,[b] Jungmok You,[d] Yusuke Yamauchi,*[d,e,f] Ahmed F. M. EL-Mahdy,*[a,g] and Shiao-Wei Kuo*[a,h]

a. Department of Materials and Optoelectronic Science and College of Semiconductor and Advanced Technology Research, National Sun Yat-Sen University, Kaohsiung, 80424, Taiwan. E-mails: ahmedelmahdy@mail.nsysu.edu.tw and kuosw@faculty.nsysu.edu.tw

b. Research Center for Materials Nanoarchitectonics (MANA), National Institute for Materials Science (NIMS), 1-1 Namiki, Tsukuba, Ibaraki 305-0044, Japan

c. Chemistry Department, Faculty of Science, Tanta University, Tanta 31527, Egypt

d. Department of Plant & Environmental New Resources, College of Life Sciences, Kyung Hee University, 1732 Deogyeong-daero, Giheung-gu, Yongin-si, Gyeonggi-do 17104, South Korea

e. Australian Institute for Bioengineering and Nanotechnology (AIBN), The University of Queensland, Brisbane, QLD 4072, Australia

f. Department of Materials Process Engineering, Graduate School of Engineering, Nagoya University, Nagoya 464–8603, Japan

g. Chemistry Department, Faculty of Science, Assiut University, Assiut 71516, Egypt

h. Department of Medicinal and Applied Chemistry, Kaohsiung Medical University, Kaohsiung 807, Taiwan

Corresponding Authors:

E-mail: TORAD.Nagy@nims.go.jp; nagi.kamal@science.tanta.edu.eg (N. L. Torad) ; y.yamauchi@uq.edu.au (Y. Yamauchi) ; ahmedelmahdy@mail.nsysu.edu.tw (A. F. M. EL-Mahdy) ; kuosw@faculty.nsysu.edu.tw (S. W. Kuo)

Table of Contents

1. Materials

All chemicals used for this study were from analytical grade and applied for experiments without further purification.

No.	Chemical name	Supplier
1	Tetrakis(triphenylphosphine)palladium ((Pd(PPh_3)$_4$)	Sigma Aldrich
2	Potassium acetate	Sigma Aldrich
3	Bis(triphenylphosphine)palladium(II) dichloride (dppf($PdCl_2$)	Sigma Aldrich
4	Dioxane	San Diego, USA
5	Tetrahydrofuran (THF)	San Diego, USA
6	Dichloromethane (DCM)	San Diego, USA
7	Dimethylformamide (DMF)	Alfa-Aesar
8	Ammonium acetate	Alfa-Aesar
9	4-bromoacetophenone	Alfa-Aesar
10	bis(pinacolato)diboron	Alfa-Aesar
11	4,7-Dibromo-2,1,3-benzothiadiazole	TCI-America
12	1,4-dibromobenzene (Bz-2Br)	TCI-America
13	2,5-dibromothiophene	TCI-America
14	Potassium dichromate ($K_2Cr_2O_7$)	TCI-America
15	Di-bromobenzaldhyde	TCI-America
16	2-(tributylstannyl)thiophene	TCI-America
17	4,7-Dibromo-2,1,3-benzothiadiazole (Tz-2Br)	TCI-America
18	*N*-bromosuccinimide	TCI-America

2. Instrumentations

Fourier-transform infrared spectrophotometer (FTIR, Thermo/Nicolet Avatar FTIR 360 spectrometer) was used to record FTIR spectra of the synthesized samples in the range of 550-4000 cm^{-1} using KBr disks. A Bruker AVANCE III-400 WB NMR spectrometer and Bruker magic angle spinning (MAS) probe were employed for obtaining the solid state ^{13}C NMR (SSNMR) and ^{1}H NMR spectra by resetting the MAS rate of 5 kHz and contact time to 2 ms using through DMSO-d_6 and $CDCl_3$ as exterior solvents and chemical shifts (δs) were detected in parts-per million (ppm). ^{13}C CP/MAS NMR spectral data were obtained through cross-polarization with MAS (CPMAS) at 75.5 MHz. JW-BK surface area and porosity analyzer were employed for measuring N_2 adsorption-desorption isotherms of the CMP samples at 77 K. The Brunauer-Emmett-Teller (BET), *t*-plot, and the nonlocalized density functional theory (NLDFT) methods were used to analyze the specific surface area and pore structural properties of the obtained CMP materials, respectively. The surface areas of the polymer CMP materials were calculated based on the BET model by using the data of adsorption branches in the relative pressure (P/P_0) range of 0.05-0.95. The morphological structure of the obtained CMP materials was identified by a field emission scanning electron microscope (FE-SEM, JEOL JSM-7610F) operated at an accelerating voltage of 5.0 kV and a transmission electron microscope (TEM, JEOL-2010 FEI Tecnai G20) equipped with field-emission microscope (JEOL, Tokyo, Japan) that was operated at high voltage of 200 kV. TA Q50 thermogravimeter helped us for collecting thermogravimetric analysis (TGA) profiles under N_2 atmosphere at a temperature range of 20-800 °C at a ramping rate of 10 °C·min^{-1}. Shimadzu Corporation U4100 Spectrophotometer was employed for recording UV-Vis absorption spectra. ICP-OES data were obtained on a Varian Vista MPX ICP Spectrometer. Zeta potential was characterized through dynamic light scattering (DLS) with Zetasizer Nano ZS90. X-ray photoelectron spectroscopy (XPS) spectra were collected through Thermo Fisher scientific ESCALAB 250 with a micro focused monochromatic Al Kα X-ray source (15 kV) and a double-focusing full 180° spherical sector electron analyzer.

3. Experimental

3.1 Synthesis of 2, 4, 6-tris(4-bromophenyl)pyridine (TPP-3Br)

Synthesis of 2, 4, 6-tris(4-bromophenyl)pyridine (TPP-3Br) was conducted as reported in our recently published work.[S1] Briefly, 4-bromoacetophenone (4.14 g, 20.8 mmol), ammonium acetate (28.0 g, 363 mmol), 4-bromobenzaldehyde (1.94 g, 10.4 mmol) and acetic acid (14.6 mL, 0.260 mmol) were mixed in a 20 mL microwave tube at a temperature and power of 220 °C and 500 W, respectively, for 45 min

(Scheme S1). After that, the tube-containing product was cooled to the ambient temperature, then was poured into water, and neutralized by saturated solution of $NaHCO_3$. Finally, TPP-3Br was extracted by dichloromethane (DCM). DCM was evaporated and final product was dried under vacuum. FTIR (KBr pellets): 3065, 1644, 1572 cm^{-1}. 1H NMR ($CDCl_3$, 25 °C): δ = 8.037 (d, 4H), 7.8 (s, 2H), 7.647 (d, 2H), 7.65 (d, 4H), 7.58 ppm (d, 2H). ^{13}C NMR ($CDCl_3$, 25 °C): 156.5, 149.5, 137.84, 137.28, 132.28, 131.82, 128.5, 123.9, 123.5, and 116.73 ppm.

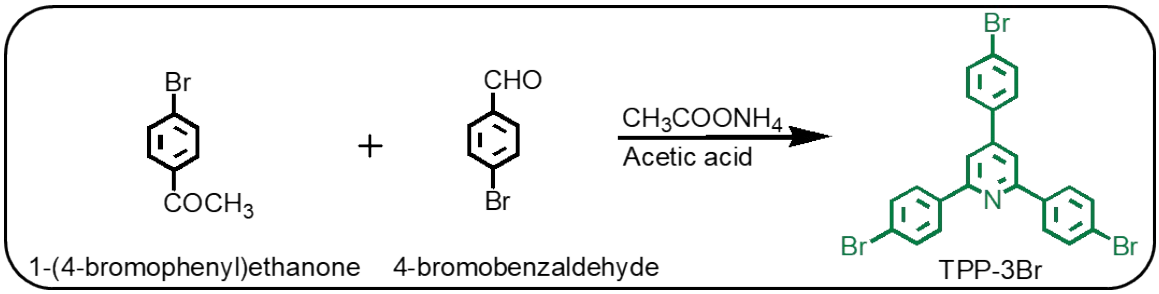

Scheme S1. Synthesis of TPP-3Br.

3.2 Synthesis of 2,4,6-tris(4-(4,4,5,5-tetramethyl-1,3,2-dioxaborolan-2-yl)phenyl)pyridine (TPP-3Bor)

2,4,6-tris(4-(4,4,5,5-tetramethyl-1,3,2-dioxaborolan-2-yl)phenyl)pyridine (TPP-3Bor) was synthesized *via* boronation process of TPP-3Br as reported earlier.[S2] Briefly, 2.57 g of bis(pinacolato)diboron (10.12 mol), 0.142 g of [1,1′-bis(diphenylphosphino)ferrocene]dichloropalladium(II) ($Pd(dppf)_2Cl_2$) (0.193 mmol) and 0.9 g of potassium acetate (9.15 mmol) was mixed a round two-neck flask (100 mL). Then, the tube-containing reactants was evacuated for 15 min. Subsequently, 50 mL of dry dioxane was injected, then the tube was kept under magnetic stirring at 110 °C for 40 h (Scheme S2). The solvent was evaporated, and the white precipitate was collected after column chromatography using THF/hexane with a ratio of 1:3 *v*/*v* as an eluent. Finally, the product was dried under vacuum at 50 °C for 10 h. The resultant product was stored in a refrigerator at 0 °C for the next step. FTIR (KBr pellets): 2980, 1613, 1534, 1399, 1212 and 1141 cm^{-1}. ^1H NMR (400 MHz, 25 °C): δ = 8.037 (*d*, J = 8.8, 4H), 7.9 (*d*, J = 8.8, 2H), 7.93 (*s*, 2H), 7.75 (*d*, 4H) 1.37 ppm (*s*, 12H). ^{13}C NMR ($CDCl_3$, 25 °C): δ = 158.4, 150.6, 142.2, 136.1, 127.7, 118.4, 84.79 and 24.69 ppm. Mass spectroscopy: 686.4 g mol^{-1}.

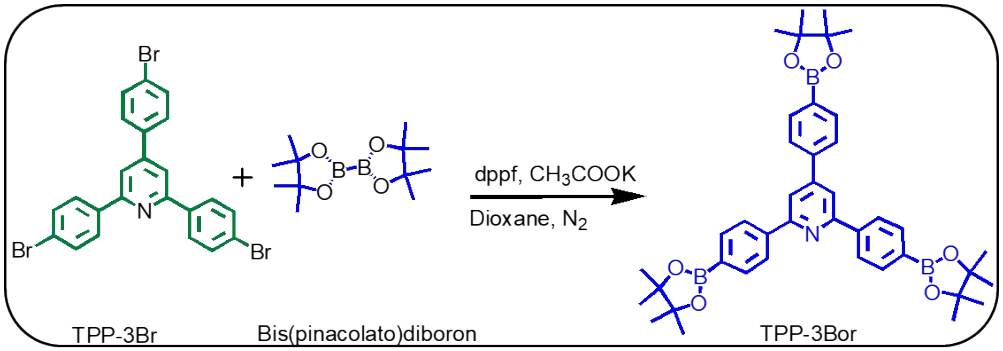

Scheme S2. The synthesis process of TPP-3Bor.

3.3 Synthesis of 4,7-di(thiophen-2-yl)benzo[c][1,2,5]thiadiazole (ThZ)

4,7-di(thiophen-2-yl)benzo[c][1,2,5]thiadiazole (ThZ) was synthesized according to an earlier report.[S3] Briefly, 4,7-Dibromo-2,1,3-benzothiadiazole (Tz-2Br) (750 mg of 2.551 mmol) and tetrakis(triphenylphosphine) palladium(0) (590 mg, 0.510 mmol) were mixed in a 100-mL round two-neck flask and the flask-containing reactants mixture was then evacuated for 15 min. After that, the reaction was conducted under N_2 atmosphere by the injection of dry *N*,*N*-Dimethylformamide (DMF, 10 mL) and 2-(tributylstannyl)thiophene (2.43 mL) into the flask, then it was left under magnetic stirring and refluxing for 72 h at 120 °C under N_2 atmosphere (Scheme S3). Finally, after solvent evaporation, an orange precipitate was formed. The precipitate was finely purified using column chromatography using DCM/hexane (1:4 *v*/*v*) eluent and silica gel. FTIR (KBr pellets): 2965, 1730, 1633, and 1261 cm^{-1}. ^1H NMR (400 MHz, 25 °C): δ = 8.13 (*d*, 2H), 7.88 (*s*, 2H), 7.47 (*d*, 2H) and 7.20 (*m*, 2H) ppm. The melting point was recorded as 120-122 °C.

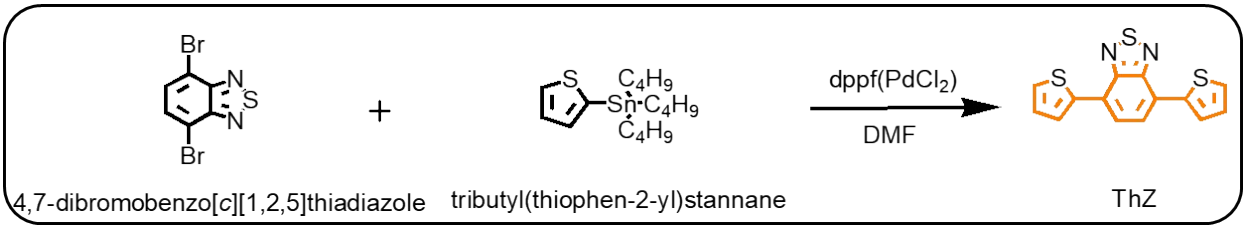

Scheme S3. The synthesis process of ThZ.

3.4 Synthesis of 4,7-bis(5-bromothiophen-2-yl)benzo[c][1,2,5]thiadiazole (ThZ-2Br)

According to an earlier report, [S3] 4,7-bis(5-bromothiophen-2-yl)benzo[c][1,2,5]thiadiazole (ThZ-2Br) was also synthesized using the as-synthesized ThZ (637 mg, 2.12 mmol) dissolved in 50 mL chloroform, followed by the addition of *N*-bromosuccinimide (831 mg) in one portion in a 100-mL two-neck flask totally covered with Al foil covered. The reaction was conducted in dark under N_2 atmosphere at room temperature for 72 h (Scheme S4). Finally, the resultant product was filtered, then washed with a copious amount of deionized water, methanol, and chloroform. The obtained red solid precipitate was dried under vacuum for 20 h. ^{1}H NMR (400 MHz, 25 °C): δ = 7.82 (*d*, 2H), 7.81 (*s*, 2H), and 7.17 (*d*, 2H) ppm. The melting point was recorded to be 252-254 °C.

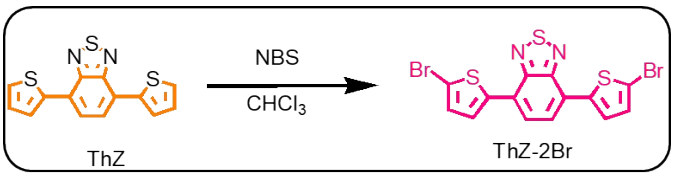

Scheme S4. The synthesis process of ThZ-2Br.

3.5 TPP-based CMPs

3.5.1 TPP-ThZ CMP

To synthesize our TPP-based CMPs, the as-synthesized 2,4,6-tris(4-(4,4,5,5-tetramethyl-1,3,2-dioxaborolan-2-yl)phenyl)pyridine (TPP-3Bor; 180 mg, 0.262 mmol) and ThZ-2Br (181 mg, 0.393 mmol) were mixed with $Pd(PPh_3)_4$ (50 mg, 0.043 mmol), and K_2CO_3 (3.93 mmol, 544 mg) in a Schlenk tube and then the reactants components were degassed for 15 min. After that, DMF (10 mL) and water (1.25 mL) were added, and the feeding tube was then treated with a triple freeze-thaw cycle. The reaction was conducted under continuous magnetic stirring at 110 °C for 72 h. The tube was cooled to room temperature and the resultant polymer was washed with deionized water, methanol, and tetrahydrofuran (THF). The solid precipitate was dried in a convection oven at 100 °C for 15 h (Scheme S5).

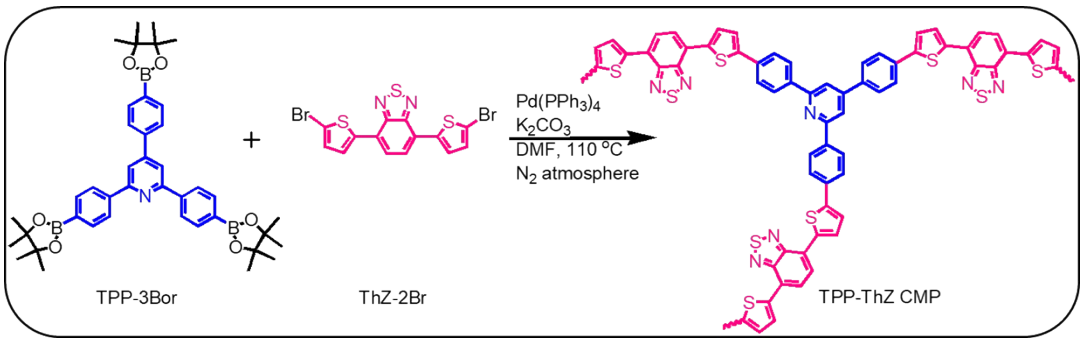

Scheme S5. The synthesis process of TPP-ThZ CMP.

3.5.2 TPP-Th CMP

The synthesis process was of TPP-Th CMP followed as the one of TPP-ThZ CMP except Th-2Br was used instead (Scheme S6). The as-synthesized 2,4,6-tris(4-(4,4,5,5-tetramethyl-1,3,2-dioxaborolan-2-yl)phenyl)pyridine (TPP-3Bor; 180 mg, 0.262 mmol) and Th-2Br monomer (95.32 mg, 0.393 mmol) were mixed with $Pd(PPh_3)_4$ (50 mg, 0.043 mmol), and K_2CO_3 (3.93 mmol, 544 mg) in a Schlenk tube and then the reactants components were degassed for 15 min. After that, DMF (10 mL) and water (1.25 mL) were added, and the feeding tube was then treated with a triple freeze-thaw cycle. The reaction was conducted under continuous magnetic stirring at 110 °C for 72 h. The tube was cooled to room temperature and the resultant polymer was washed with deionized water, methanol, and tetrahydrofuran (THF). The solid precipitate was dried in a convection oven at 100 °C for 15 h (Scheme S6).

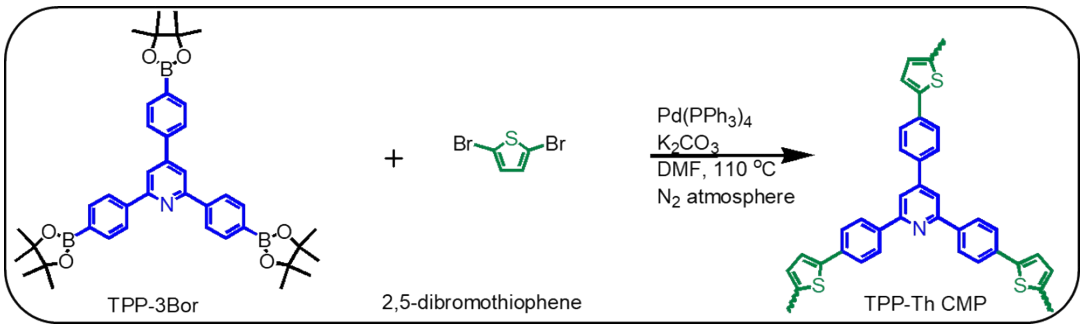

Scheme S6. The synthesis process of TPP-Th CMP.

3.5.3 TPP-Bz CMP

The synthesis process was of TPP-Th CMP followed as the one of TPP-ThZ CMP except Bz-2Br was used instead (Scheme S7). The as-synthesized 2,4,6-tris(4-(4,4,5,5-tetramethyl-1,3,2-dioxaborolan-2-yl)phenyl)pyridine (TPP-3Bor; 180 mg, 0.262 mmol) and Bz-2Br (96.2 mg, 0.404 mmol) were mixed with $Pd(PPh_3)_4$ (50 mg, 0.043 mmol), and K_2CO_3 (3.93 mmol, 544 mg) in a Schlenk tube and then the reactants components were degassed for 15 min. After that, DMF (10 mL) and water (1.25 mL) were added, and the feeding tube was then treated with a triple freeze-thaw cycle. The reaction was conducted under continuous magnetic stirring at 110 °C for 72 h. The tube was cooled to room temperature and the resultant polymer was washed with deionized water, methanol, and tetrahydrofuran (THF). The solid precipitate was dried in a convection oven at 100 °C for 15 h (Scheme S7).

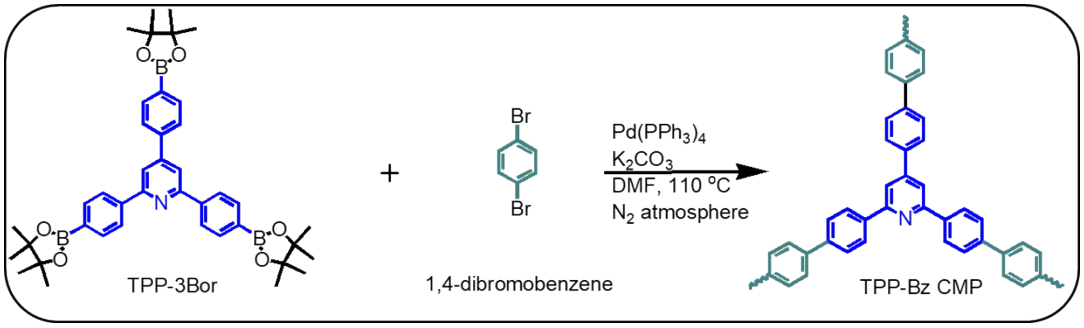

Scheme S7. The synthesis process of TPP-Bz CMP.

3.6 Detoxification experiments

3.6.1 Kinetics studies of adsorption

Standard solutions of Cr(VI) were prepared from $K_2Cr_2O_7$ in deionized water. The experiments were performed in 3 mL glass vials at room temperature (295 K). A series of batch experiments were carried out to determine the performance conditions of the CMPs adsorbents for the adsorptive-reduction of hazardous Cr(VI) to Cr(III). Each experiment was repeated three times to estimate the average adsorption capacities at different pH 2. The equilibrium adsorption capacities of CMPs for Cr (VI) were set at the generally accepted value of three times the value of the counting error. The TPP-based CMP adsorbent (6 mg, 2 g L^{-1}) was mixed thoroughly with a standard solution of Cr(VI) (3 mL, 50 mg L^{-1}). Then, the suspension solution was stirred at 350 rpm for predetermined different time intervals (between 5 min and 150 h) at 295 K. The solution was quickly centrifuged at 6000 rpm and the supernatant was withdrawn by a syringe into the quartz-cuvette. The initial and final concentration of each metal ion were determined by UV-Vis absorption spectroscopy by measuring the absorbance at $\lambda = 350$ nm. The ICP-AES measurements were conducted to quantify the trace elements at low levels after adsorptive-reduction of Cr(VI). The solution pH was adjusted in the range of pH 1-8 using aqueous solutions of HCl (0.1 M) and NaOH (3.0 M) with a pH meter to study the effect of pH on the adsorption performance of the TPP-based CMPs adsorbents.

The adsorption capacities (Q_e, mg g^{-1}) and removal efficacies (%) of the TPP-based CMPs were calculated from the change in Cr concentration during the adsorption process according to estimated according to Eqn. (S1 and S2):

$$Q_e = (C_i - C_t)^{v}/_{m} \ldots\ldots\ldots\ldots\ldots\ldots\ldots\ldots (Eqn.S1)$$

$$Removal\ efficacy\ (\%) = (C_i - C_e)/C_i \times 100 \ldots\ldots\ldots\ldots (Eqn.S2)$$

Where, Q_e is the equilibrium adsorption, C_i , C_t and C_e are the initial concentration, the concentration at time (*t*) and at equilibrium. m describes the weight of the adsorbent (g) and v is the volume of the solution (L).

To investigate the adsorption kinetics of Cr(VI) over TPP-based CMP adsorbent, the procedures followed were the same as those given in the above-mentioned experimental procedure. The solid–liquid separation process and the determination of Cr concentrations were conducted as described above. The potential rate-controlling steps involved in the adsorption of Cr into CMP adsorbents was investigated and

the pseudo-first-order, pseudo-second-order and intraparticle-diffusion were applied to fit the experimental data.

3.6.2 Isotherm studies of adsorption

For equilibrium adsorption isotherm, TPP-based CMP adsorbent (5 mg, 1.6 g L^{-1}) was mixed with different standard solutions of hexavalent Cr(VI) (3 mL, initial concentrations: 50, 75, 100, 150, 200 mg L^{-1} at pH 2 and room temperature. The suspension solution was then stirred magnetically overnight under the same conditions described above. The stability experiments were performed using TPP-based CMPs (5 mg, 1.6 g L^{-1}) dispersed in hexavalent Cr(VI) (6 mL, 50 mg L^{-1}) solutions and stirring at room temperature for 5 h to ensure the full adsorption of toxic hexavalent Cr(VI) ions. The solution was quickly centrifuged at 6000 rpm and the supernatant was withdrawn by a syringe into the quartz-cuvette. The initial and final concentration of each metal ion were determined by UV-Vis absorption spectroscopy by measuring the absorbance at λ = 350 nm.

4. Supporting results and discussions

4.1 Characterization of monomers

The TPP-3Br was synthesized as depicted in Scheme S1.[S1] The FTIR spectrum displays multi-signals at 3065, 1644, and 1572 cm^{-1}, corresponding to the aromatic C−H, C=N, and C=C groups, respectively (Fig. S1). Furthermore, the ^{1}H NMR profile of TPP-3Br shows the presence of doublet peaks at 8.03, 7.64, 6.65-7.58 ppm and another singlet peak at 7.80 ppm, which is attributed to protons of pyridyl ring and the substituted aryl rings (Fig. S6). Moreover, ^{13}C NMR profile of TPP-3Br displays multi signals at 156.51, 149.52, and 116.70 ppm, assignable to carbon nuclei of the pyridyl ring, and the other characteristic peaks of aryl substituents were shown at 137.84, 132.28, 131.82, 123.90 and 123.50 ppm. On the other hand, boronated form of TPP-3Br (TPP-3Bor) was achieved *via* simple boronation reaction of TPP-3Br, which is revealed by the stretching vibrations of C−H, C=N, C=C, B−O, C−B and C−O located at 2980, 1613, 1534, 1399, 1212 and 1141 cm^{-1}, respectively, as depicted by FTIR in Fig. S1. Furthermore, the ^{1}H NMR spectrum of the TPP-3Bor represents a characteristic singlet peak at 1.37 ppm, which reveals the presence of CH_3 groups of boron rings. The presence of ^{1}H NMR peaks located at 8.03, 7.93, 7.90 and 7.75 ppm are assignable to the pyridyl ring and aryl substituents as shown in Fig. S7. The ^{13}C NMR spectrum of TPP-3Bor revels the presence of carbon nuclei peaks of boron ring at 24.69 and 84.79 ppm. In addition, six characteristic peaks located at 158.4, 150.6, 142.2, 136.1, 127.7 and 118.4 ppm are assignable to

pyridyl ring and aryl rings (Fig. S10). The molecular formula of TPP-3Bor is determined from the mass spectroscopy spectrum in Fig. S11.

The FTIR spectrum of ThZ molecule represents the existence of several characteristic bands at 2965, 1730, and 1633 cm^{-1}, assignable to the stretching vibrations of C−H, C=N, and C=C, respectively. The band at 1261 cm^{-1} is characteristic of C-H bending vibration (Fig. S2). The ^{1}H NMR spectrum of ThZ clarifies the proton peaks of carbon nuclei at 8.13 ppm due to aryl rings. The presence of peaks at 7.88, 7.47 and 7.22 ppm reveals the formation of thiophene rings, which is much consistent with the recently published report (Fig. S8).[S3] ThZ monomer is considered as the starting material for synthesizing ThZ-2Br through a simple bromination step using *N*-bromosuccinimide (NBS). The FTIR spectrum of ThZ-2Br reveals the formation characteristic bands located at 3026, 1706 and 1636 cm^{-1}, corresponding to the stretching vibrations of C−H, C=N and C=C, respectively, in addition to the bending vibration of C−H group existed at 1307 cm^{-1} (Fig. S2). The ^{1}H NMR spectrum of ThZ-2Br clarifies the presence of three characteristic signals at 7.82, 7.81, and 7.17 ppm, assignable to the protons of aryl and thiophene rings, which is consistent with the recently published report (Fig. S9).[S3]

4.1.1 FTIR spectra

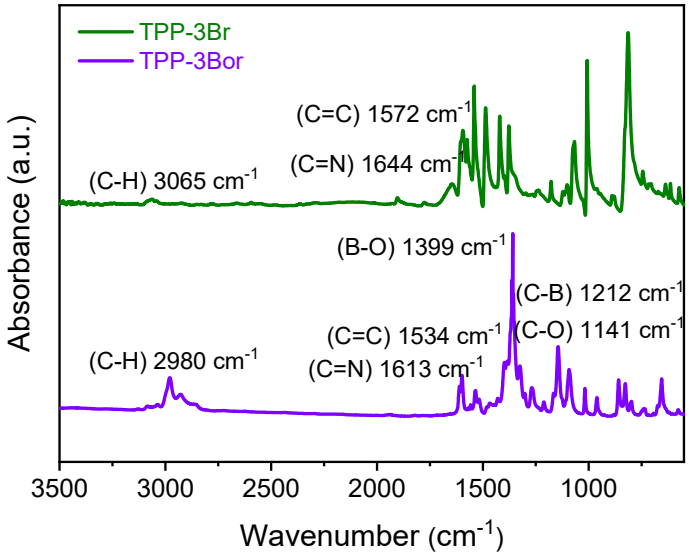

Fig. S1. The FTIR spectra of TPP-3Br, and TPP-3Bor.

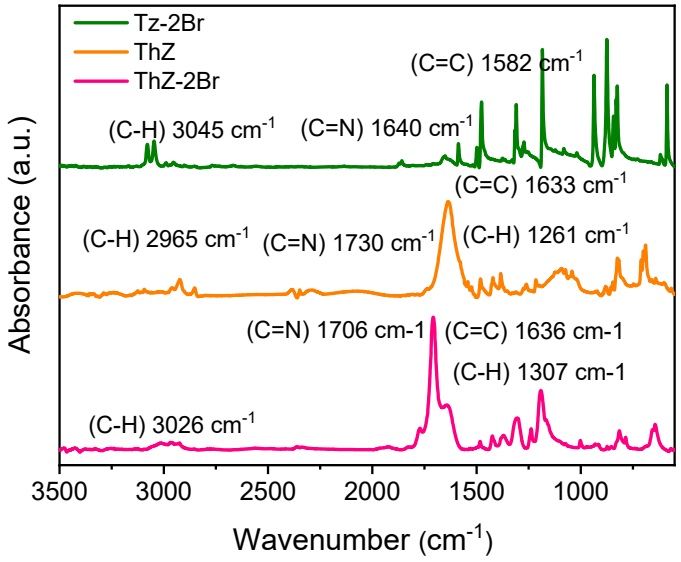

Fig. S2. The FTIR spectra of Tz-2Br, ThZ, and ThZ-2Br.

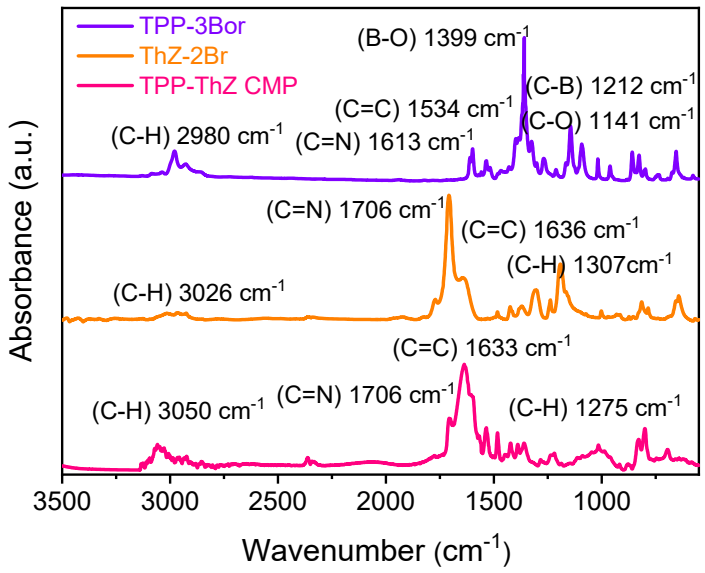

Fig. S3. The FTIR spectra of TPP-3Bor, ThZ-2Br and TPP-ThZ CMPs.

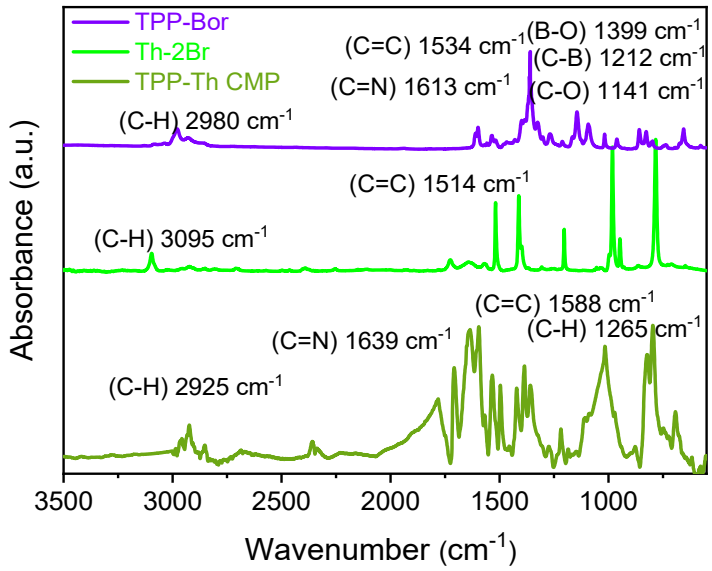

Fig. S4. The FTIR spectra of TPP-3Bor, Th-2Br and TPP-Th CMPs.

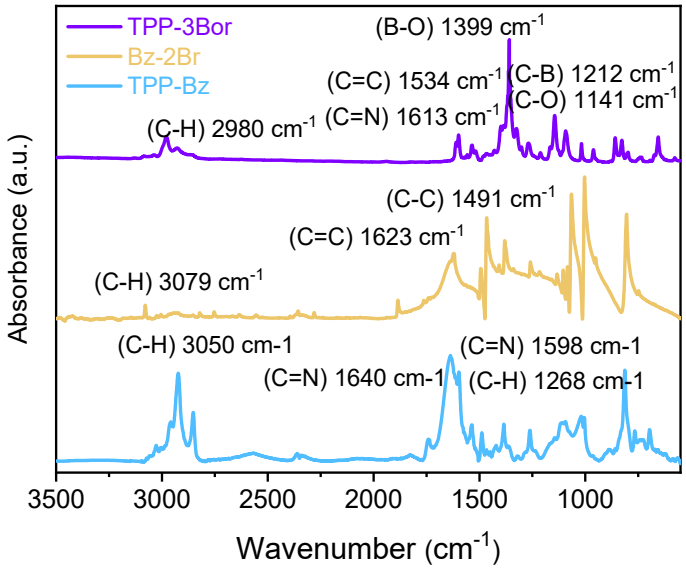

Fig. S5. The FTIR spectra of TPP-3Bor, Bz-2Br and TPP-Bz CMPs.

4.1.2 NMR spectra

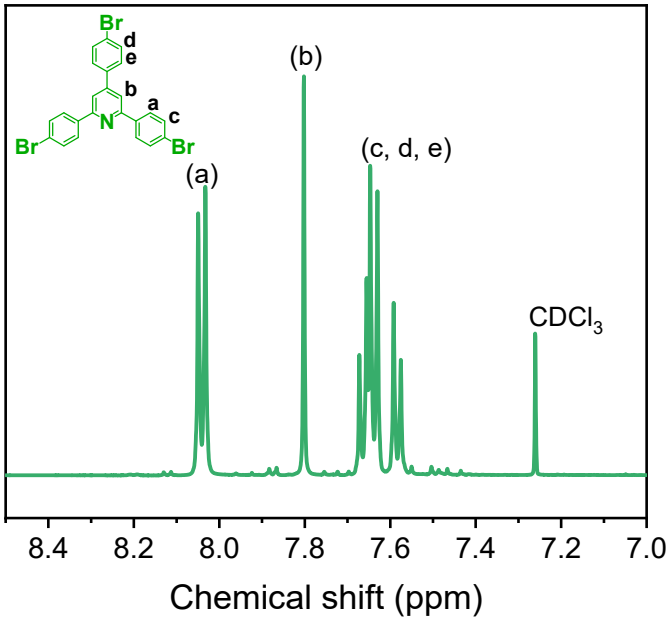

Fig. S6. The ^{1}H NMR spectrum of TPP-3Br.

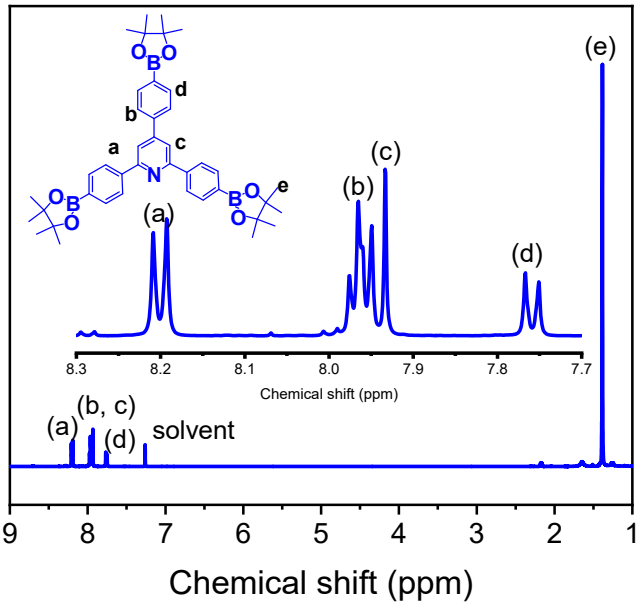

Fig. S7. The ^{1}H NMR spectrum of TPP-3Bor.

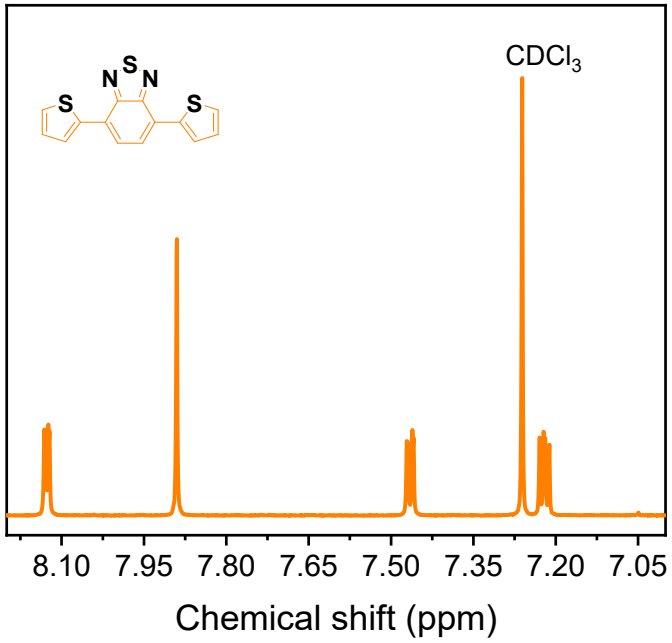

Fig. S8. The ^{1}H NMR spectrum of ThZ.

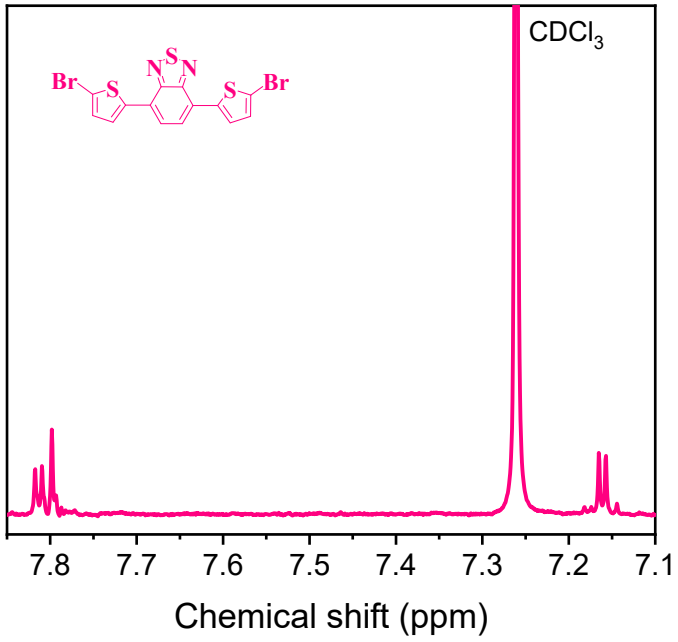

Fig. S9. The ^{1}H NMR spectrum of ThZ-2Br.

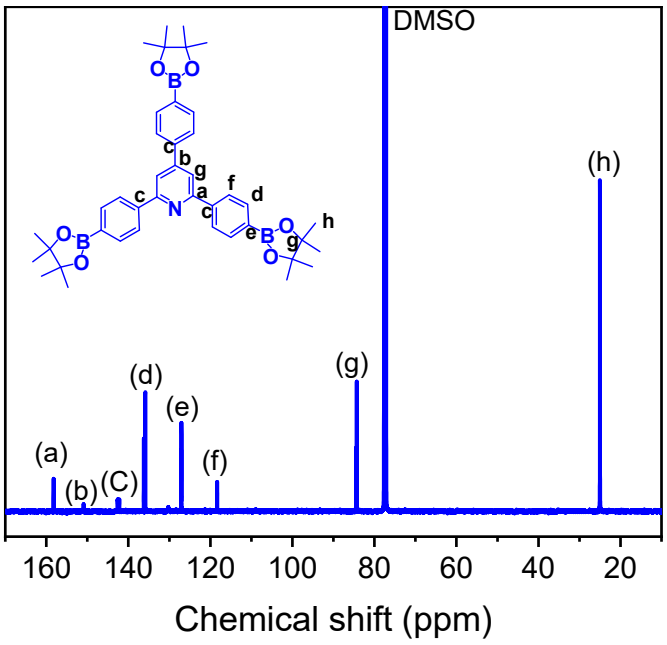

Fig. S10. The ^{13}C NMR spectrum of TPP-3Bor.

4.1.3 Mass spectroscopy spectrum

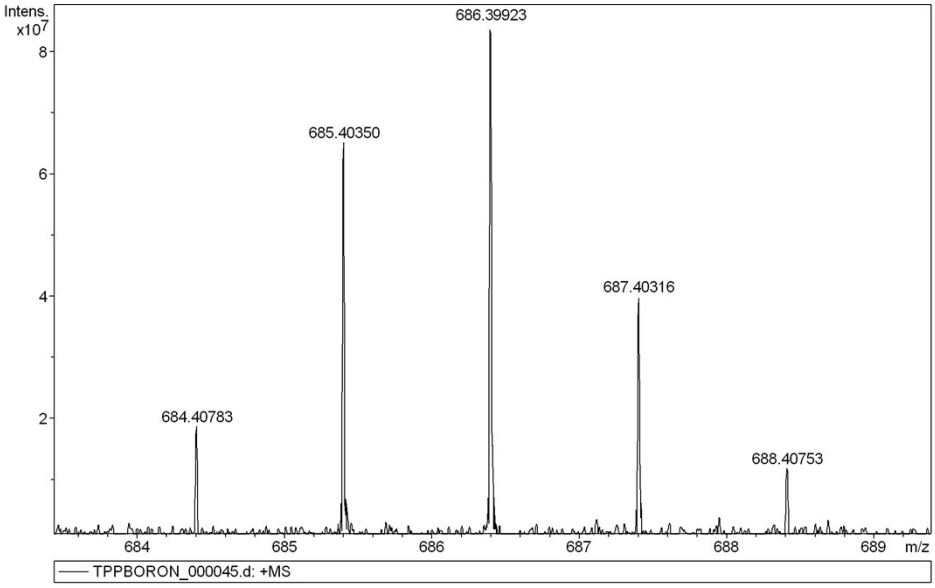

Fig. S11. The mass spectroscopy of TPP-3Bor.

4.2 TGA analysis

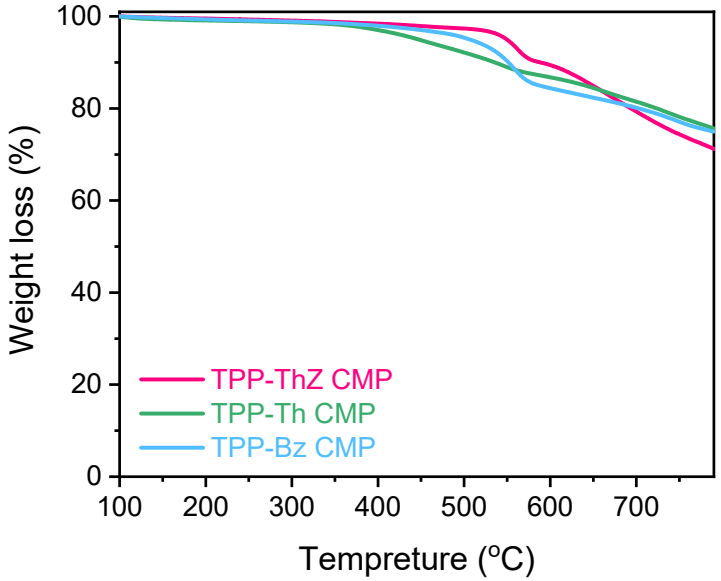

Fig. S12. TGA analysis of TPP-ThZ, TPP-Th, and TPP-Bz CMPs.

4.3 UV-Vis absorption measurements

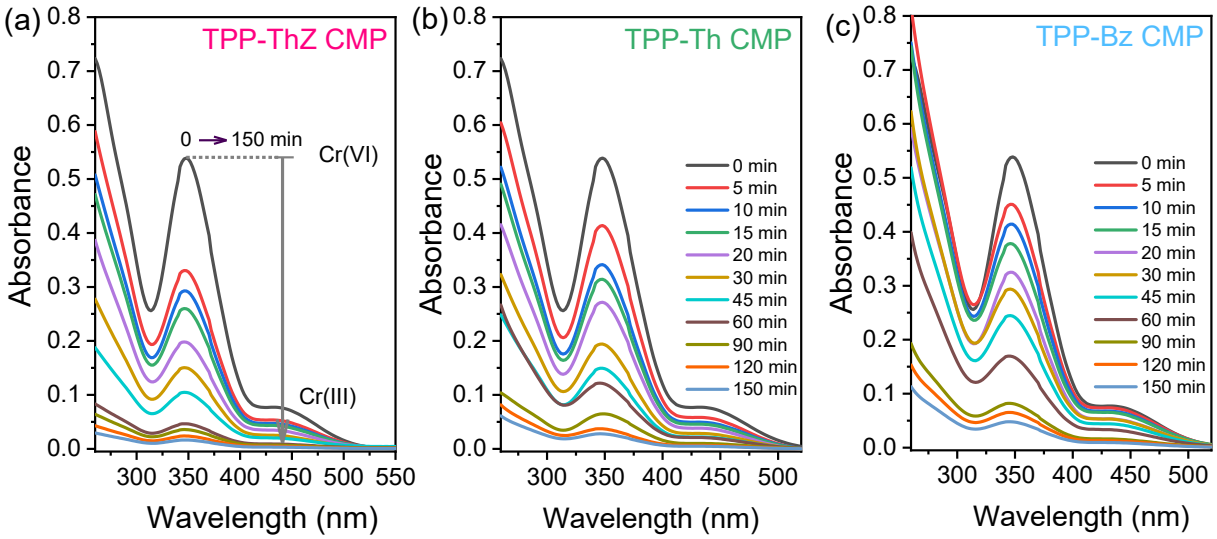

Fig. S13. The effect of the contact time on the adsorption properties of (a) TPP-ThZ, (b) TPP-Th and (c) TPP-Bz CMPs. The weight of the CMP sample is 6 mg and Cr(VI) solution is 50 mg L^{-1} at pH 2 under room temperature.

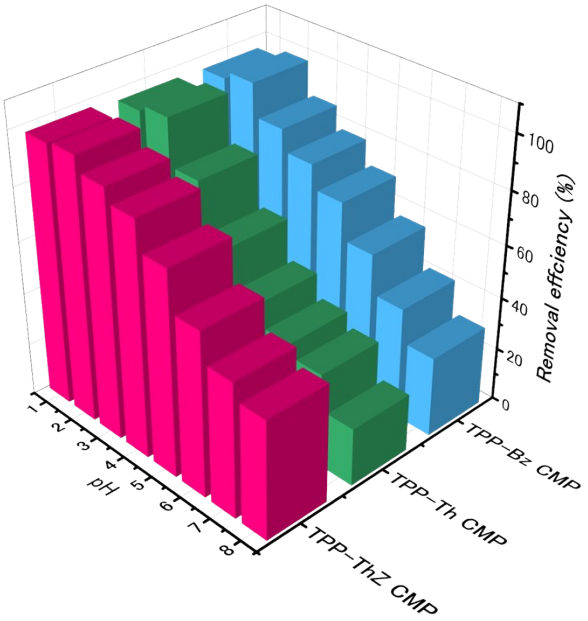

Fig. S14. Removal efficacy of Cr(VI) ions in a wide ranges of pH media.

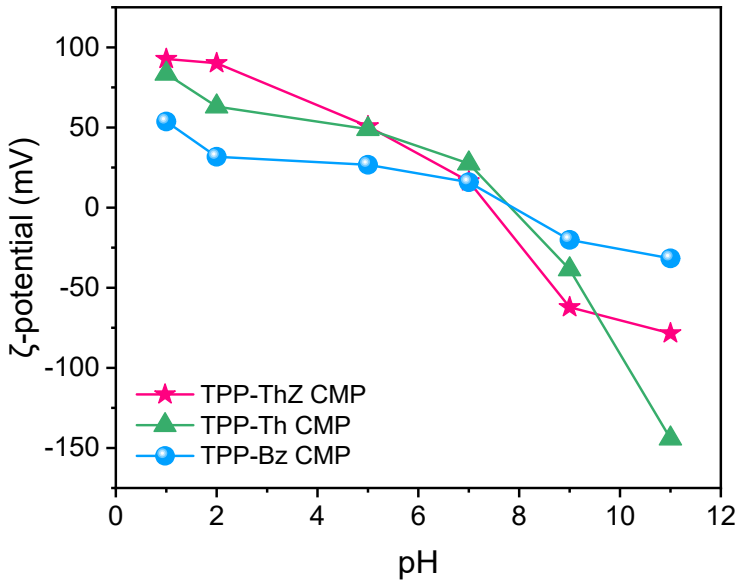

Fig. S15. Zeta-potential measurement of TPP-ThZ, TPP-Th, and TPP-Bz CMPs over a wide range of pH media.

Table S1. Binding energy and relative content (%) of C1s for the TPP-based CMPs adsorbents before and after Cr(VI) adsorption.

Valence state	Carbon states	TPP-ThZ CMP		TPP-Th CMP		TPP-Bz CMP	
		Before adsorption	After adsorption	Before adsorption	After adsorption	Before adsorption	After adsorption
C1s	C=C	32.38%	30.83%	28.61%	27.86%	22.91%	21.16%
	C=N	43.79%	42.19%	49.82%	47.36%	54.38%	49.56%
	C-S	23.83%	26.98%	21.57%	24.78%	--	--
	C=O					19.15%	24.39%
	π-π*					3.56%	4.89%

Table S2. Kinetic parameters of pseudo-first-order, pseudo-second-order and intraparticle diffusion kinetics models.

Samples	Pseudo-first order			Pseudo-second order			Intraparticle diffusion		
	Q_e (mg g^{-1})	k_1 (min^{-1})	R^2	Q_e (mg g^{-1})	k_2 (g mg^{-1} min^{-1})	R^2	K_i	C (mg L^{-1})	R^2
TPP-ThZ CMP	24.87	0.0487	0.975	30.35	1.34×10^{-3}	0.994	2.08	3.20	0.95
TPP-Th CMP	23.48	0.0312	0.927	28.10	1.29×10^{-3}	0.976	2.02	0.974	0.98
TPP-Bz CMP	21.91	0.0295	0.832	26.90	0.90×10^{-4}	0.985	1.90	0.12	0.97

Table S3. Isotherm parmeters of Langmuir and Freendulish isotherms models.

Samples	Langmuir isotherm				Freundlich isotherm			
	Q_{max} (mg L^{-1})	K_L (L g^{-1})	Intercept	R^2	K_F ($L^{1/n}$ $mg^{1/n-1}$ g^{-1})	n	Intercept	R^2
TPP-ThZ CMP	209.20	0.1562	0.03061	0.991	44.25	2.656	0.18522	0.976
TPP-Th CMP	118.20	0.529	0.01598	0.999	43.26	4.115	0.24301	0.916
TPP-Bz CMP	84.80	0.193	0.06090	0.996	34.54	5.398	0.37639	0.995

Table S4. Comparative study of TPP CMPs toward Cr(VI) removal with recent adsorbents.

Materials	Dose ($g\ L^{-1}$)	Initial Concentration ($mg\ L^{-1}$)	Q_m ($mg\ g^{-1}$)	Eq. time (min)	Ref.
Aniline formaldehyde condensate (AFC) salt (Poly-1s)	4.0	100	98.00	NA	S4
Lignosulfonate	NA	NA	57.14	300.0	S5
Activated carbon	4.0	10	3.460	40.00	S6
Polyaniline (PANI) aerogel	15	50	41.20	300.0	S7
Pyrogenic carbon hybrid	1.0	50	36.12	500.0	S8
Almandine/humboldtine nanospheres composites	0.4	1.0	48.23	100.0	S9
Acrylamide-thiosemicarbazide cellulose (ATC)	4.0	20	83.40	1200	S10
Modified carbonized coal (CTAB/CC) composite	NA	NA	78.67	NA	S11
Short chain polyaniline (PANI)-jute	2.0	10	3.520	NA	S12
Aniline formaldehyde condensate (AFC)-based silica gel	8.0	10	0.620	180.0	S13
Chitosan-graphene oxide nanocomposite	5.0	10	1.960	NA	S14
Micron size AFC	2.0	10	4.500	NA	S15
Cellulosed based anion exchanger	2.0	10	4.99	60.00	S16
Nanocrystalline akageneite	NA	NA	80.00	90.00	S17
Polyacrylonitrile fibers	1.0	50	35.00	120.0	S18
Chitosan coated with poly 3-methyl thiophene	100	NA	127.62	NA	S19
Graphite N and thiophene S of N, S-co-doped hydrochar derived from waste straw (SNHC)	1	100	171.33	NA	S20
TPP-ThZ CMP	1.6	50	209.2	60.00	**This study**
TPP-Th CMP	1.6	50	118.2	90.00	
TPP-Bz CMP	1.6	50	84.80	150.0	

4.4 Stabilities measurements

4.4.1 SSNMR measurements

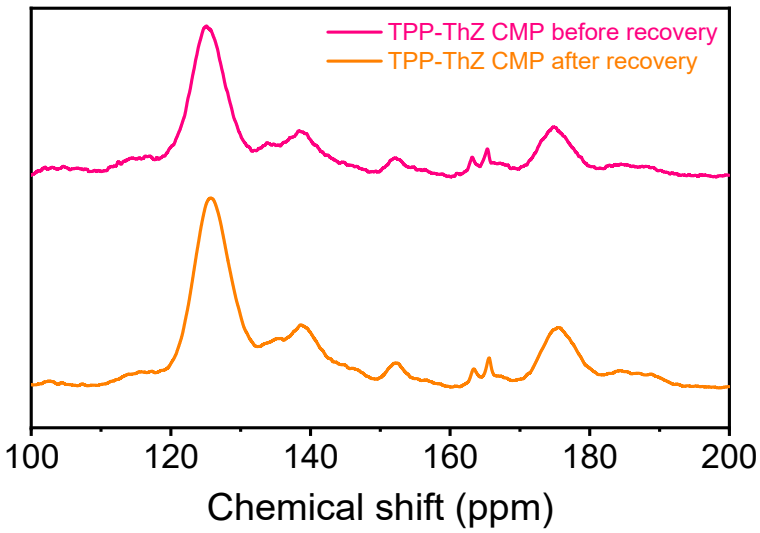

Fig. S16. SSNMR of TPP-ThZ CMP before and after Cr(VI) adsorption.

4.4.2 Morphological studies using SEM and TEM measurements

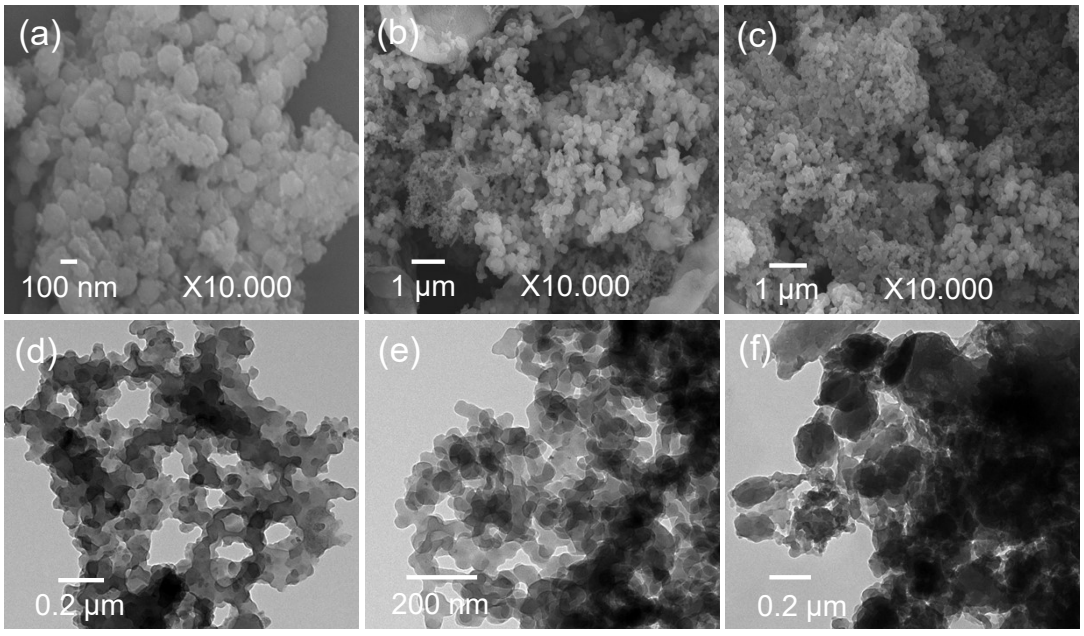

Fig. S17. SEM and TEM images of (a,d) TPP-ThZ, (b, e) TPP-Th, and (c, f) TPP-Bz after adsorption removal of Cr(VI).

5. References

S1 A. F. M. El-Mahdy, C.-H. Kuo, A. Alshehri, C. Young, Y. Yamauchi, J. Kim and S.-W. Kuo, J. Mater. Chem. A, 2018, **6**, 19532-19541.

S2 M. G. Kotp, A. M. Elewa, A. F. M. El-Mahdy, H.-H. Chou and S.-W. Kuo, ACS Appl. Energy Mater., 2021, **4**, 13140-13151.

S3 V. H. Fell, N. J. Findlay, B. Breig, C. Forbes, A. R. Inigo, J. Cameron, A. L. Kanibolotsky and P. J. Skabara, J. Mater. Chem. C, 2019, **7**, 3934-3944.

S4 T. Dutta and M. Ray, Chem. Eng. J., 2022, **431**, 133368.

S5 J. Geng, F. Gu and J. Chang, J. Hazard. Mater., 2019, **375**, 174-181.

S6 S. Karnjanakom and P. Maneechakr, J. Mol. Struct., 2019, **1186**, 80-90.

S7 S. Zaghlol, W. A. Amer, M. H. Shaaban, M. M. Ayad, P. Bober and J. Stejskal, Chem. Pap., 2020, **74**, 3183-3193.

S8 M. Zhao, C. Zhang, X. Yang, L. Liu, X. Wang, W. Yin, Y. C. Li, S. Wang and W. Fu, J. Hazard. Mater., 2020, **396**, 122712.

S9 Q. Zeng, Y. Huang, H. Wang, L. Huang, L. Hu, H. Zhong and Z. He, J. Hazard. Mater., 2020, **383**, 121199.

S10 R. Pei, Q. Li, J. Liu, G. Yang, Q. Wu, M. Wu, S. Tong, Y. Lv, X. Ye and Y. Liu, J. Polym. Environ., 2020, **28**, 2199-2210.

S11 M. K. Seliem and M. Mobarak, J. Mol. Liq., 2019, **294**, 111676.

S12 P. A. Kumar, S. Chakraborty and M. Ray, Chem. Eng. J., 2008, **141**, 130-140.

S13 P. A. Kumar, M. Ray and S. Chakraborty, J. Hazard. Mater., 2007, **143**, 24-32.

S14 M. E. Ali, Arab. J. Chem., 2018, **11**, 1107-1116.

S15 P. Terangpi, S. Chakraborty and M. Ray, Chem. Eng. J., 2018, **350**, 599-607.

S16 T. Anirudhan, S. Jalajamony and P. Suchithra, Colloids Surf. A Physicochem. Eng. Asp., 2009, **335**, 107-113.

S17 N. Lazaridis, D. Bakoyannakis and E. Deliyanni, Chemosphere, 2005, **58**, 65-73.

S18 S. Deng and R. Bai, Water Res., 2004, **38**, 2424-2432.

S19 S. Hena, J. Hazard. Mater., 2010, **181**, 474-479.

S20 Y. Liu, T. Wang, N. Song, Q. Wang, Y. Wu, Y. Zhang and H. Yu, Sci. Total Environ., 2023, **860**, 160360.